Journal of Power Technologies 103 (3) (2023) 138 -- 145

Closed loop ĈUK topology based single-phase high-performance AC-DC converter

Md. Ismail Hossain[1*]✉ and Dr. Mohammad Jahangir Alam[1]
[1]Department of Electrical and Electronic Engineering BUET, Dhaka-1000, Bangladesh
✉ jewel04eee@yahoo.com

Abstract

This paper focluses on the analysis of a power factor correction (PFC) converter using close loop Ĉuk topology. Regardless of the input line voltage and output load variations, input current drawn by the buck or buck-boost converter is always discontinuous. The boost converter suffers from high voltage stresses across the power electronic devices. The input current in Ĉuk converter is comparable to boost converter's input current. In this paper output voltage is controlled by inner current and outer voltage control loop along with power factor correction (PFC). It shows less input current THD (less than 5%), attains nearly unity power factor and better output voltage regulation of AC-DC converter under variable input voltage and output load. Small signal model analysis is presented for obtaining frequency response of the control loop. The MATLAB Simulink programming environment is used as a simulation tool.
Keywords: PWM, state space averaging technique, small signal model, Ĉuk topology, voltage loop and current loop etc.

1. Introduction

The use of computers and telecommunications equipment have become important in our society. Electric vehicles are rapidly increasing in use due to their environmentally friendly technology. DC power supply is the quintessential part of these devices and in most cases, it comes from AC-DC converter. The efficiency, total harmonic distortion of input current, input power factor and regulated output voltage etc. are the main concerns of these AC-DC converters.

Uncontrolled diode rectifiers followed by L-C smoothing filters are widely used as a cheap power supply. Uncontrolled charging of DC filter capacitor results in 50Hz pulsed AC current waveform at the input of the rectifier. Several power quality problems arise at the source side, which include poor power factor, high input current total harmonic distortion (THD), failure of transformers due to overheating and harmonic pollution on grid [1-2] etc. Grid disturbances may result in malfunction or damage of electrical devices. Many methods for elimination of harmonic pollution in the power system are in use and new methods are being investigated. Restrictions on current and voltage harmonics are maintained in many countries through IEEE 519-1992 and IEC 61000-3-2/IEC 61000-3-4[3] standards. The restrictions are associated with the idea of "clean power". The power factor correction (PFC) converter topology using active wave shaping techniques can overcome the problem in line current. The PFC converter forces the line to draw near sinusoidal AC current in phase with its voltage.

Most of the single-phase AC to DC conversion PFC work is done with buck, boost, and buck-boost or fly-back topology between the source and the load. Buck and buck-boost topology suffer from input discontinuous current [4-7]

and boost topology needs large value capacitance [8] to minimize the output voltage ripple therefore initial inrush current is higher than Ĉuk converter [9-10]. Ĉuk converter requires low value intermediate capacitance to transfer energy to output capacitance and load [9-10]. In this paper output voltage and input current control variable duty cycle Ĉuk converter has been proposed for minimizing output voltage variation due to line voltage and load variation and obtaining sinusoidal AC mains current. Fixed frequency is chosen due to easier parameter design compared to hysteresis control.

2 Proposed close loop Ĉuk regulator-based AC-DC converter

Proposed close loop Ĉuk regulator based ACDC converter is shown in Fig. 1. The technique used here is the average current mode control. In average current mode control, the output voltage is controlled by varying the average value of the current signal. The voltage feed forward compensator controls the input voltage variation in such a way that if the input voltage reduces then the output of voltage feed forward compensator increases and vice versa. The actual output DC voltage is sensed and compared with a reference voltage then the voltage error is processed through the proportional integral controller. The output of the proportional integral controller is multiplied with the rectified input voltage and output of voltage feed forward compensator to make a reference current in phase with rectified input voltage. The real current is forced to track the reference current through current error compensator. The error between the actual current and reference current is processed through the proportional integral controller and then its output is compared with the sawtooth wave to generate the required PWM signal.

3 Close loop response analysis of AC–DC Ĉuk converter using state space averaging technique

For analysis the stability of the proposed control system using bode plot open loop transfer function is needed. For continuous conduction mode (CCM), DC-DC converters operate in two circuit states in one switching period, (i) when switch is on for a time interval dT and (ii) when switch is off for a time interval (1-d) T, where d is a duty cycle and T is switching period. According to Le Verrier Algorithm modeling of DC-DC converters using SSA method needs three steps in general as discussed below.

a. During each circuit state, the linear circuit is described by the state variable vector x. Generally, inductor currents and capacitor voltages are chosen as state variables. The state space equations of two circuit states, in standard form, are obtained as switch is on during time interval dT, state-space equations of converter can be written as:

$$\frac{dx(t)}{dt} = A_1 x(t) + B_1 u(t) \text{ and } y(t) = C_1 x(t) + E_1 u(t) \quad (1)$$

The matrices A_1, B_1, C_1 and E_1 describe the network connections during the time interval dT. $x(t)$, $u(t)$ and $y(t)$ are the state variable, input variable and output variable respectively. When switch is off during time interval $(1-d)T$, state-space equations of converter can be written as:

$$\frac{dx(t)}{dt} = A_2 x(t) + B_2 u(t) \text{ and } y(t) = C_2 x(t) + E_2 u(t) \quad (2)$$

The matrices A_1, B_1, C_1 and E_1 describe the network connections during the time interval $(1-d)T$. Equation (1) and (2) are time weighted and averaged over one switching period as:

$$\frac{dx(t)}{dt} = A_{12}x(t) + B_{12}u(t) \text{ and}$$
$$y(t) = C_{12}x(t) + E_{12}u(t), \quad (3)$$

where:

$$A_{12} = A_1 d + A_2(1-d), B_{12} = B_1 d + B_2(1-\mathrm{d})$$

$$C_{12} = C_1 d + C_2(1-d), E_{12} = E_1 d + E_2(1-\mathrm{d})$$

b. Now linearization is produced by introducing small AC perturbation around a DC operating point. To obtain a small signal AC model around a quiescent operating point, the following small perturbation as shown in equation (4) is added to state space model represented by equation (3),

$$x(t) = X + \tilde{x}(t), y(t) = Y + \tilde{y}(t)$$
$$u(t) = U + \tilde{u}(t), d(t) = D + \tilde{d}(t) \quad (4)$$

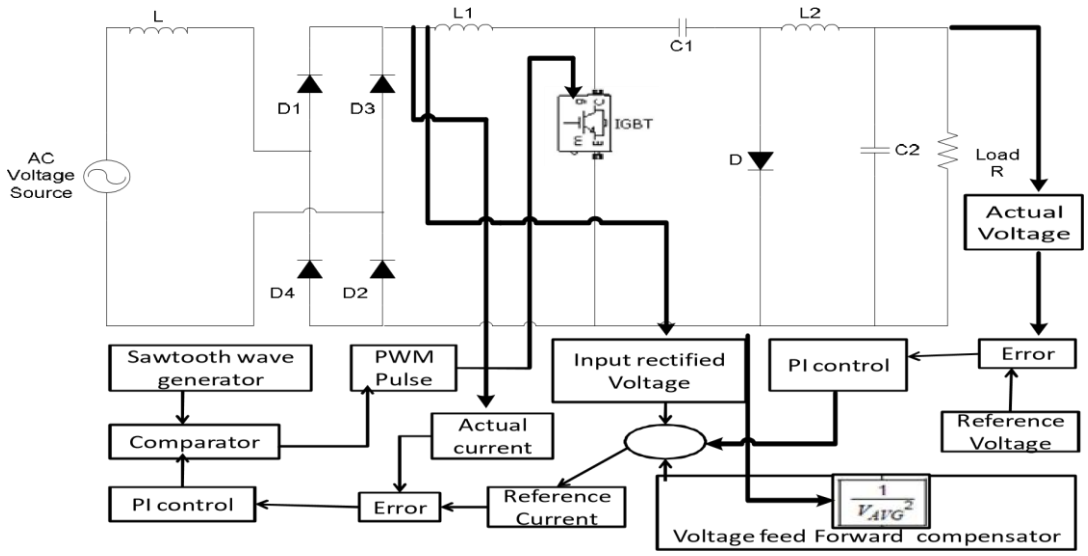

Figure 1: Proposed close loop Ćuk regulator-based AC-DC converter

The capital letter represents a DC value. Small signal linearization is justified under the following condition:
$X > \tilde{x}(t), Y > \tilde{y}(t), U > \tilde{u}(t)$ and $D > \tilde{d}(t)$.

Now replacing equation (3) in equation (4) we can get a small signal state space model as

$$\frac{d\tilde{x}(t)}{dt} = A\tilde{x}(t) + B\tilde{u}(t) + B_d\tilde{d}(t)$$
$$\tilde{y}(t) = C\tilde{x}(t) + E\tilde{u}(t) + E_d\tilde{d}(t), \quad (5)$$

where:

$$A = A_1 D + A_2(1-D), B = B_1 D + B_2(1-D)$$
$$C = C_1 D + C_2(1-D), E = E_1 D + E_2(1-D)$$
$$B_d = [(A_1 - A_2)X + (B_1 - B_2)U]$$
$$E_d = [(C_1 - C_2)X + (E_1 - E_2)U].$$

Taking Laplace transform of equation (5) we have:

$$\tilde{X}(s) = (sI - A)^{-1}\left[B\tilde{u}(s) + B_d\tilde{d}(s)\right] \quad (6)$$

$$\tilde{Y}(s) = C(sI - A)^{-1}\left[B\tilde{u}(s) + B_d\tilde{d}(s)\right] + E\tilde{u}(s) + E_d\tilde{d}(s) \quad (7)$$

Using equation (6) and (7) for *DC* value of input voltage $V_{IN,}$ output voltage V_O and duty cycle *D*, the control-to-output and the input-to-output small signal transfer functions of the converter are respectively given as:

$$\frac{\widetilde{V_O}(s)}{\tilde{d}(s)} = C(sI - A)^{-1}B_d + E_d \quad (8)$$

$$\frac{\widetilde{V_O}(s)}{\widetilde{V_{IN}}(s)} = C(sI - A)^{-1}B + E \quad (9)$$

Now for Ĉuk converter in Figure Figure 2 the parameter A_1, B_1, C_1 and E_1 is derived by the following way when switch is on for dT time then from Figure Figure 2 (a) we have:

$$\frac{diL1}{dt} = \frac{V_{\text{rect}}\ \text{average}}{L1}, \frac{diL2}{dt} = \frac{VC1 - V}{L2}$$
$$\frac{dVC1}{dt} = \frac{-iL2}{C1}, \frac{dVC2}{dt} = \frac{iL2 - \frac{VC2}{R}}{C2} \quad (10)$$
$$V_{\_\text{out}} = -VC2$$

When switch is off for $(1-d)T$ time then from Figure Figure 2 (b) we have:

$$\frac{diL1}{dt} = \frac{-VC1 + V_{\text{rect\_average}}}{L1}$$
$$\frac{diL2}{dt} = \frac{-VC2}{L2}, \frac{dVC1}{dt} = \frac{iL1}{C1} \quad (11)$$
$$\frac{dVC2}{dt} = \frac{iL2 - \frac{VC2}{R}}{C2}, V_{\_\text{out}} = -VC2$$

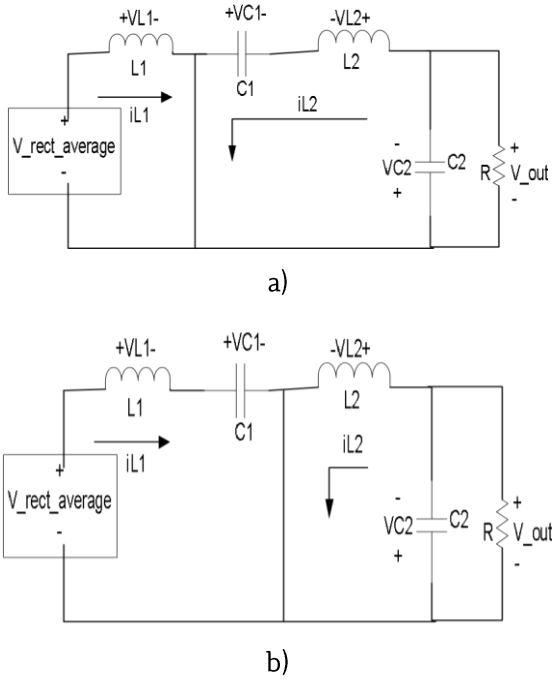

Figure 2: Ĉuk converter (a) when switch is closed (b) when switch is opened

Therefore:

$$A_1 = \begin{vmatrix} 0 & 0 & 0 & 0 \\ 0 & 0 & \frac{1}{L2} & \frac{-1}{L2} \\ 0 & \frac{-1}{C1} & 0 & 0 \\ 0 & \frac{1}{C2} & 0 & \frac{-1}{RC2} \end{vmatrix}, B_1 = \begin{vmatrix} \frac{1}{L1} \\ 0 \\ 0 \\ 0 \end{vmatrix}, \quad (12)$$
$$C_1 = |0 \quad 0 \quad 0 \quad -1| \text{ and } E_1 = [0].$$

$$A_2 = \begin{vmatrix} 0 & 0 & \frac{-1}{L1} & 0 \\ 0 & 0 & 0 & \frac{-1}{L2} \\ \frac{1}{C1} & 0 & 0 & 0 \\ 0 & \frac{1}{C2} & 0 & \frac{-1}{RC2} \end{vmatrix}, B_2 = \begin{vmatrix} \frac{1}{L1} \\ 0 \\ 0 \\ 0 \end{vmatrix}, \quad (13)$$
$$C_2 = |0 \quad 0 \quad 0 \quad -1| \text{ and } E_2 = [0].$$

So, using the state space averaging method we have:

$$A = \begin{vmatrix} 0 & 0 & \frac{-D}{L1} & 0 \\ 0 & 0 & \frac{D}{L2} & \frac{-1}{L2} \\ \frac{D'}{C1} & \frac{-D}{C1} & 0 & 0 \\ 0 & \frac{1}{C2} & 0 & \frac{-1}{RC2} \end{vmatrix}, B = \begin{vmatrix} \frac{1}{L1} \\ 0 \\ 0 \\ 0 \end{vmatrix}, \quad (14)$$
$$C = |0 \quad 0 \quad 0 \quad -1|, E = [0].$$

$$B_d = \begin{vmatrix} \frac{V\_rect\_average}{D/L1} \\ \frac{V\_rect\_average}{D/L2} \\ \frac{-V\_rect\_averageD}{RC1D/2} \end{vmatrix} \text{ and } E_d = 0 \quad (15)$$

4 Stability analysis of the controller using Bode plot

The main objective of the control system is to draw a sinusoidal current, in phase with the input voltage. The reference inductor current $i_L^*(t)$ as shown in Figure Figure 3 is of the full wave rectified form. The requirements on the form and the amplitude of the inductor current lead to two control loops as shown in Figure

Figure 3 to pulse width modulate the switch of the Ćuk converter.

The inner current loop ensures the form of $i_L^*(t)$ based on the input voltage. The outer voltage loop determines the amplitude i_L^* of $i_L^*(t)$ based on the output voltage feedback. If the inductor current is insufficient for a given load supplied by the control system, the output voltage will drop below its pre-selected reference value V_d^*. By measuring the output voltage and using it as the feedback signal the voltage loop adjusts the inductor current amplitude to bring the output voltage to its reference value. In addition to determining the inductor current amplitude, this voltage feedback control acts to regulate the output voltage to the preselected DC voltage. In order to follow the reference with as little THD as possible, an average current mode control is used with a high bandwidth, where the error between the reference $i_L^*(t)$ and the measured inductor current $i_L(t)$ is amplified by a current controller to produce the control voltage $v_c(t)$ and finally gives PWM signal. The current control loop and voltage control loop are shown in Figure Figure 4 and Figure Figure 5 respectively. The open loop transfer function of the current loop is:

$$T_{I(s)} = H1(s)H2(s)H3(s), \qquad (16)$$

where $H1(s) = K_{pI} + \frac{K_{iI}}{S}$ *and* $H2(s) = \frac{1}{v_r}$;

$$H3(s) = \frac{2.121 \times 10^{-12}S^2 - 8.094 \times 10^7 S^2 + 2.576 \times 10^{12}S - 2.76 \times 10^{16}}{S^4 + 1.887S^3 + 9{,}849 \times 10^8 S^2 + 1.641 \times 10^9 S + 1.55 \times 10^{13}}$$

The open loop transfer function of the voltage loop is:

$$T_{V(s)} = H4(s)H5(s)H6(s), \qquad (17)$$

where $H4(s) = K_{pV} + \frac{K_{iV}}{S}$ *and* $H5(s) = 1$;

$$H6(s) = \frac{2.196 \times 10^{-12}S^7 - 2.961 \times 10^7 S^6 - 2.965 \times 10^{12}S^{57} - 2.192 \times 10^{17}S^4 - 2.471 \times 10^{22}S^3 - 2.3 \times 10^{26}S^2 + 3.997 \times 10^{25}S + 3.198 \times 10^{30}}{2.221 \times 10^4 S^7 + 1.073 \times 10^9 S^6 + 2.71 \times 10^{14}S^5 + 8.943 \times 10^{18}S^4 + 7.154 \times 10^{23}S^3 + 3.7 \times 10^{24}S^2 + 9.947 \times 10^{27}S + 3.314 \times 10^{28}}$$

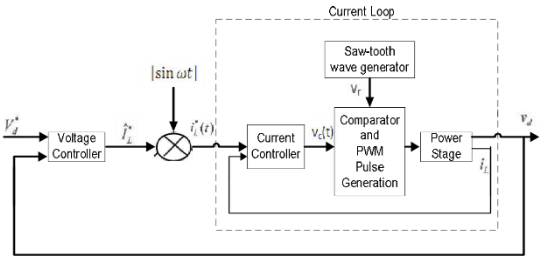

Figure 3: Control loop of the proposed control system

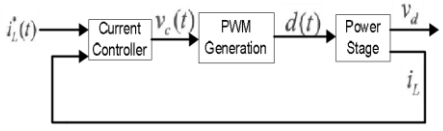

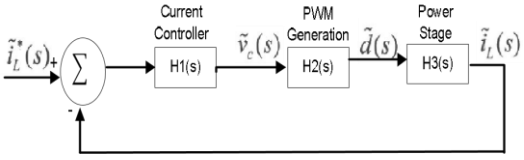

Figure 4: Current loop of the control system

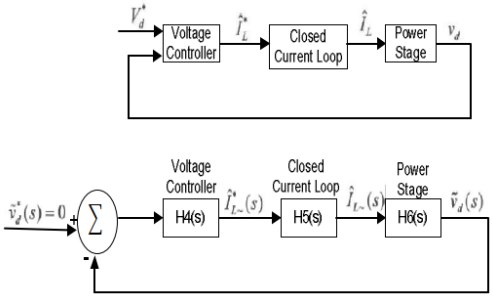

Figure 5: Voltage loop of the control system

5 Simulation in MATLAB Simulink

L=100*uH*, *L1*=10*mH*, *L2*=5*mH*, *C1*=0.1*uF*, *C2*=1500*uF* and switching frequency = 80000*Hz* are used for simulation.

For voltage loop K_p=27 and K_i = 0.1 and for current loop K_p=0.2 and K_i = 0.4 are used. Figure Figure 6 shows the Bode plot of transfer function TV(s) and TI(s). Figure Figure 7 to Figure Figure 10 show the reference /real current, input voltage/current/output voltage, input current THD, power factor/efficiency respectively for 400Ω load resistance and -400*V* reference voltage under 325*V* (peak) input

voltage and 50Hz supply frequency. Figure Figure 11 to Figure Figure 13 show the dynamic response due to load and input voltage disturbance.

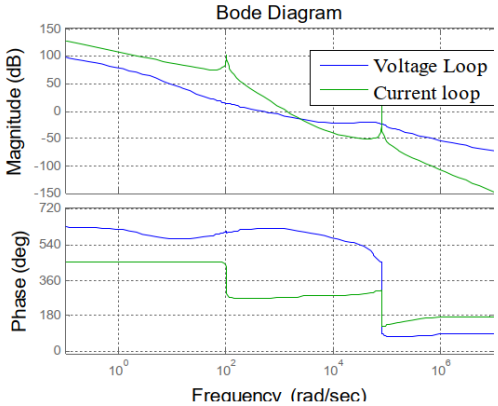

Figure 6: Stability analysis of voltage/current loop using bode plot

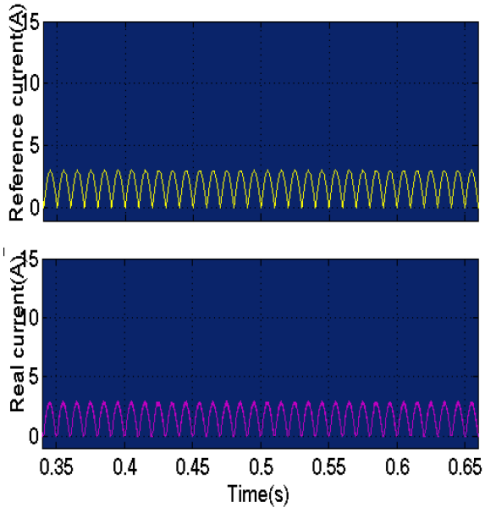

Figure 7: Reference and real current for 400 Ω load

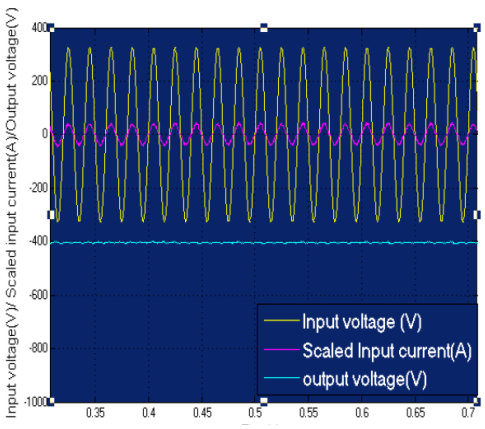

Figure 8: Input voltage, input current and output voltage for 400 Ω load

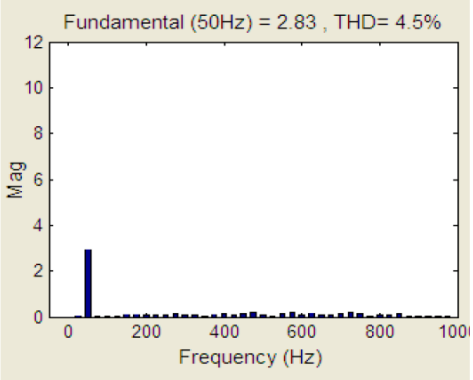

Figure 9: FFT analysis of input current

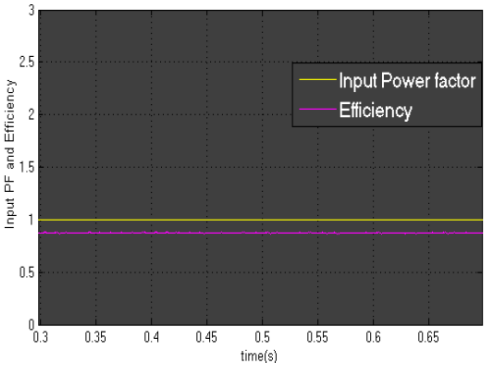

Figure 10: Input power factor and efficiency

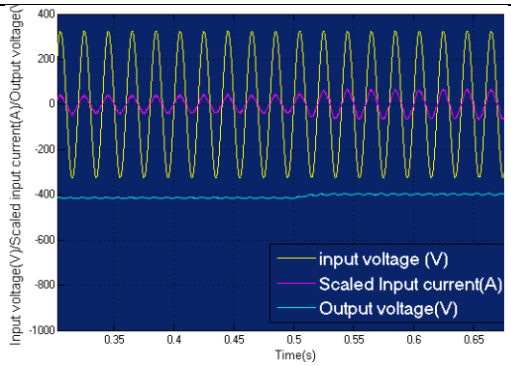

Figure 11: Dynamic input voltage, input current and output voltage after load changed from 250W to 400W at 0.5s

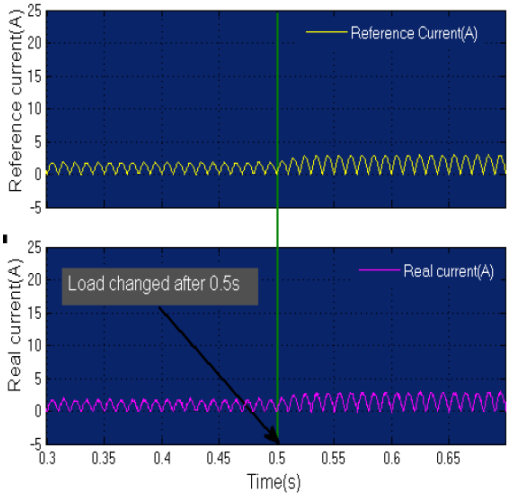

Figure 12: Dynamic reference and real current after load changed from 250W to 400W at 0.5s

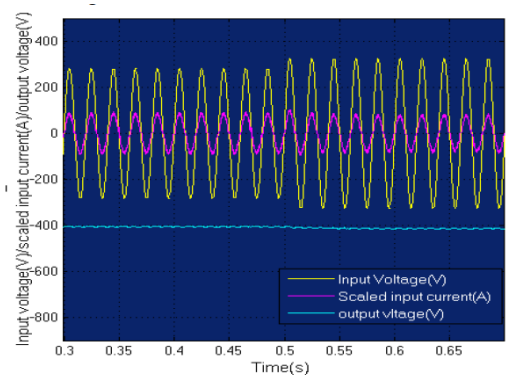

Figure 13: Dynamic input voltage, input current and output voltage after input voltage changed from 200V(rms) to 230V(rms)

6 Conclusion

The use of outer voltage and inner current control loop in Ĉuk topology-based AC-DC converter is analyzed and implemented in this paper where simulations result in Matlab Simulink are described. The results show how well this controller improves the input current THD, input power factor and output voltage regulation under the variable load and input voltage disturbance.

References

[1] Zixin Li, Yaohua Li, Ping Wang, Hai bin Zhu, Cong wei Liu and Wei Xu," Control of Three-Phase Boost-Type PWM Rectifier in Stationary Frame under Unbalanced Input Voltage" IEEE Trans. On Power Electronics, VOL. 25, NO.10, OCTOBER 2010, pp. 2521-2530.

[2] Thomas Nussbaumer and Johann W. Kolar "Comparison of 3-Phase Wide Output Voltage Range PWM Rectifiers", IEEE Tran on Power electronics, VOL.54, NO.6, DECEMBER 2007. pp. 3422-3425.

[3] H. Azizi and A.Vahedi, "Performance Analysis of Direct Power Controlled PWM Rectifier under Disturbed AC Line Voltage", ICREPQ'05, 15-16-17 March 2005, Zaragoza- Spain Serial 244, 2005 pp.1-6.

[4] Ray-Lee Lin and Rui-Che Wang, "Noninverting Buck-Boost Power-Factor Correction Converter with Wide Input Voltage-Range Applications", IECON 2010, Page(s): 599 –604.

[5] Mahadev S. Patil, "Single phase buck type power factor corrector with lower harmonic contents in compliances with IEC 61000-32", International Journal of Engineering Science and Technology Vol. 2(11), 2010, pp.6122-6130.

[6] Majid Jamil and Zahra Mehdi, "Power factor improvement of cascaded buck boost converter" National power electronics conference (NPEC-10), Indian Institute of Technology Roorkee june-2010, pp.1-6.
[7] Wang Wei, "A novel bridgeless buck-boost PFC converter" Power Electronics Specialists Conference, 2008. PESC 2008. IEEE Page(s): 1304 – 1308.
[8] K. Periyasamy, "Power Factor Correction Based on Fuzzy Logic Controller with Average Current-Mode For DC-DC Boost Converter", International Journal of Engineering Research and Applications (IJERA) Vol. 2, Issue 5, September- October 2012, pp.771-777.
[9] Muhammad H. Rashid "Power Electronics Handbook 3rd edition devices circuits and application" Elsevier Inc, Burlington USA, 2011.
[10] Bimal k. Bose "Modern Power electronics and AC drives" Prentice Hall PTR, Upper saddle river 2002.